



**HAL**  
open science

# Improved Aerodynamics of a Hollow-Blade Axial Flow Fan by Controlling the Leakage Flow Rate by Air Injection at the Rotating Shroud

Michael Pereira, Florent Ravelet, Kamel Azzouz, Tarik Azzam, Hamid Oualli, Smaine Kouidri, Farid Bakir

► **To cite this version:**

Michael Pereira, Florent Ravelet, Kamel Azzouz, Tarik Azzam, Hamid Oualli, et al.. Improved Aerodynamics of a Hollow-Blade Axial Flow Fan by Controlling the Leakage Flow Rate by Air Injection at the Rotating Shroud. 13th International Conference on Computational Heat Mass and Momentum Transfer (ICCHMT 2021), 2021, Paris (on line), France. hal-03182828

**HAL Id: hal-03182828**

**<https://hal.science/hal-03182828>**

Submitted on 26 Mar 2021

**HAL** is a multi-disciplinary open access archive for the deposit and dissemination of scientific research documents, whether they are published or not. The documents may come from teaching and research institutions in France or abroad, or from public or private research centers.

L'archive ouverte pluridisciplinaire **HAL**, est destinée au dépôt et à la diffusion de documents scientifiques de niveau recherche, publiés ou non, émanant des établissements d'enseignement et de recherche français ou étrangers, des laboratoires publics ou privés.

# Improved Aerodynamics of a Hollow-Blade Axial Flow Fan by Controlling the Leakage Flow Rate by Air Injection at the Rotating Shroud

Michael Pereira, Florent Ravelet, Kamel Azzouz, Tarik Azzam, Hamid Oualli, Smaine Kouidri, Farid Bakir

► **To cite this version:**

Michael Pereira, Florent Ravelet, Kamel Azzouz, Tarik Azzam, Hamid Oualli, et al.. Improved Aerodynamics of a Hollow-Blade Axial Flow Fan by Controlling the Leakage Flow Rate by Air Injection at the Rotating Shroud. ICCHMT (on line), 2021, Paris, France. hal-03182828

**HAL Id: hal-03182828**

**<https://hal.archives-ouvertes.fr/hal-03182828>**

Submitted on 26 Mar 2021

**HAL** is a multi-disciplinary open access archive for the deposit and dissemination of scientific research documents, whether they are published or not. The documents may come from teaching and research institutions in France or abroad, or from public or private research centers.

L'archive ouverte pluridisciplinaire **HAL**, est destinée au dépôt et à la diffusion de documents scientifiques de niveau recherche, publiés ou non, émanant des établissements d'enseignement et de recherche français ou étrangers, des laboratoires publics ou privés.

## Improved Aerodynamics of a Hollow-Blade Axial Flow Fan by Controlling the Leakage Flow Rate by Air Injection at the Rotating Shroud.

Michael PEREIRA<sup>1</sup>, Florent RAVELET<sup>1</sup>, Kamel AZZOUZ<sup>2</sup>, Tarik AZZAM<sup>3</sup>, Hamid OUALLI<sup>3</sup>, Smaïne KOUIDRI<sup>1</sup>, and Farid BAKIR<sup>1</sup>

<sup>1</sup>Arts et Metiers Institute of Technology, CNAM, LIFSE, HESAM University, F-75013 Paris, France

<sup>2</sup>Valeo Thermal System, Advanced Engineering, Thermal & Thermodynamics, 78322, France

<sup>3</sup>Ecole Militaire Polytechnique (EMP), Laboratory of Fluid Mechanics, 16111, Algiers, Algeria

### Abstract

Axial flow fans are used in many fields in order to ensure the mass and heat transfer from air, chiefly in HVAC industry. A more proper understanding of the airflow behavior through the systems is necessary to manage and optimize the fan operation. Computational Fluid Dynamics (CFD) represent a real tool providing the ability to access flow structures in areas where measuring equipment cannot reach. Reducing the leakage flow rate, inherent in operation by synthetic-jet techniques improves performance. This paper presents the CFD results performed on a hollow blade fan developed by our team. The leakage flow is controlled by blowing air from 16 designated circular holes and arranged on the fan shroud. We discuss the results for two rotational speeds (1000 and 2000 rpm) and two injection rates (0.4 and 0.8). The numerical results consistent with the experimental show, for the low rotation speed and high injection ratio, significant gains in power (53%), torque (80%) and leakage flow rate (80%).

**Keywords:** Axial flow fan, CFD, Leakage flow rate, air injection, hollow blade, rotating shroud.

### Nomenclature

$C_0$	torque without control	$\dot{m}_{gap_0}$	leakage flow gap rate without control
$C$	torque with control	$\dot{m}_{gap}$	leakage flow gap rate with control
$C_{net}$	net torque	$\Delta P$	pressure difference generated by the fan (Pa)
$Gain$	power gain added by the control	$\xi$	injection rate
$P$	power delivered by the fan (W)	$\Phi$	diaphragm diameter (m)
$P_0$	power delivered by the fan for $q_{inj} = 0$	$x_{fan}$	relative position between the fan and the carter (m)
$q_{inj}$	injection rate $m^3 \cdot s^{-1}$	$x_{holes}$	position of the injection holes on the casing (m)
$q_{max}$	maximum fan flow rate $m^3 \cdot s^{-1}$		
$q_v$	fan flow rate $m^3 \cdot s^{-1}$		
$R_{int}$	hub radius (m)		
$R_{max}$	tip radius (m)		

### Introduction:

The leakage flow rate developed in the operating set has shown a great influence on the turbomachines. This flow induced by the pressure difference either between the upper and lower surfaces of the blades, or between the upstream and downstream side of the device, is responsible for the energy losses and the generation of noise. It is in this context that the authors plan to analyze the mechanisms generated by such devices. Boudet et al. [1] have numerically and experimentally investigated the leakage flow rate for an axial fan. They showed that the major contribution of sound emission is induced by the tip vortex. For a turbine, Fischer et al. [2] were managed to characterize the structure of the tip vortex by using a modulable frequency Doppler Effect velocity meter with high temporary resolution. Pogorelov et al. [3] attempted to identify this structure for an axial fan. It shows that the reduction in the dimension of the tip clearance leads to the reduction in both the size of the tip vortex and the amplitude of the noise. Throughout an LES investigation, You et al. [4] emphasized and confirmed that the effect of this dimensions on noise generation and vibration. Lee et al. [5] discussed the influence of the height of the squealer rims for a turbine. A reduction of around 11.6% was obtained for the total pressure drop coefficient.

To reduce the leakage flow rate, various geometric solutions have been proposed. Wallis et al. [6] have dealt with the extraction of the work during the passage of the leakage flow through small vanes bladelets or turning device placed on the shell in the presence of radial barriers fixed on the casing. They managed to reduce the tangential component of the leakage flow. However, they highlighted the unsteadiness and complex structural effects of the flow at the tip clearance. Corsini et al. [7] studied the shape of the endplates placed at the end of the blades in order to change the orientation and the formation of the tip vortex. Aktürk et al [8]

improve the performance and reduction of leakage flow rate of an axial fan by means of the study of the five platform extensions of the profile on the lower surface.

Pardowitz et al. [9] employed a rotating shroud for clearance vorticity suppression. Longhouse [10] was able to reduce noise and improve efficiency by using a rotating shroud attached to the blade tips. This device prevents the formation of the vortex tip. In addition, it is a solution envisaged in so far as we want to maintain a fairly large clearance between the fan and the housing. For electric motors, cooling is generated by a centrifugal rotor, Vad el al. [11] redesigned the reference rotor by adding a shroud. For the same cooling performance, it reduces fan noise and power consumption. In addition, some geometric solutions focus on optimizing labyrinthine joints. Schramm [12] presented an optimization method for the labyrinth seal in the aim of reducing the leakage flow.

This article is dedicated to the study of the leakage rate for an axial cooling fan of an automobile engine. We study flow control by injection. Several authors have sought to improve the performance of turbomachines by means of this technique. By injection upstream of the rotor of a transonic compressor, Weigl et al. [13] succeeded in stabilizing the rotary stall and surge with an expansion of the operating range. Even at the profile scale, Rhee et al. [14] increased the lift of an injection hydrofoil near the trailing edge.

Eberlinc et al. [15, 16, 17] managed to increase the coefficient of the total pressure by 6% of an axial fan composed of hollow vanes by injection near the level of the trailing edge at the end. The jet, which is caused from the hub by an internal flow line, allowed the control of the boundary layer by increasing the local velocity and reducing the effect of the adverse pressure gradient.

Neuhaus et al [18] manage to reduce the leakage rate and improve performance

with an injection rate of 0.8%. In addition, these improvements were noted for a pulsed injection synchronized with the rotation of the fan. They achieve with an injection rate of 1.5% to widen the operating range of the fan by 62% by pushing the stall point towards low flow rates. At the displaced point, the improvement in pressure is approximately 40%.

The study by Morris and Foss [19] was devoted to the automobile cooling fan with a large clearance dimension (2.5 cm). Performance improvements were obtained for large flow rates by injection air from fixed shroud to the tip clearance.

Niu et al [20] obtained a reduction in the leakage rate using the effect of injection from different configuration of a row of 10 equidistant holes, oriented 45 ° to the end face of a turbine blades.

For shrouded fan, Buisson et al [21] study a new casing treatment, which consists on helicoidal grooving of casing. The obtained results show reduction both of 45% in leakage flow rate and 2.3% in static efficiency, and the increase of 0.4% in torque.

In this study, we investigate experimentally and numerically the effect of the active flow control by air injection in the tip clearance of axial flow cooling fan. This fan is obtained with the rotational molding process, which involve hollow shape for the whole fan (hub, blades and shroud ring). The main aim of this work is to use the hollow shape induced by this process in order to exploit it in the control of tip clearance flow by steady air injection through rotating shroud ring, which is

composed of injection holes oriented in such a way to reduce both of leakage flow rate and of the torque. With specific drive system realized at the LIFSE laboratory of Arts et Metiers Institute of Technology and adequate CFD modeling, the obtained results show reduction in leakage flow and gain in the torque.

## Experimental setup

### Blade geometry

In this study, we use an axial-flow cooling hollow fan developed by the rotational molding process using polyethylene material (figure 1) [22, 23], where the preliminary researches have been developed at Arts & Metiers. This fan was generated following a controlled vortex designed axial-flow [24]. It has six blades, tip radius  $R_{max}=179\text{mm}$ , hub-to-tip radius ratio ( $R_{int}/R_{max}$ ) equal to 0.337. A hollow circular shroud ring of 31mm length and 9mm thickness was added to ensure the increase of the fan solidity. The leakage gap is about 4mm. Figure 2 present the position of the injection holes at the middle of the shroud ring and the position between the fan and the carter ( $x_{fan}=0$ ) used in this study. these positions was investigated and their impact on the fan characteristics are not presented in this paper. The casing has a thick 46 mm.

For injection operating condition, we use the injection rate  $\xi$ , defined as :  $\xi = q_{inj}/q_{max}$ , where  $q_{inj}$  is the injection rate delivered by the drive system and  $q_{max} = 1000 \text{ l/min}$  is the maximum injection rate for the fan resistance to the internal flow.

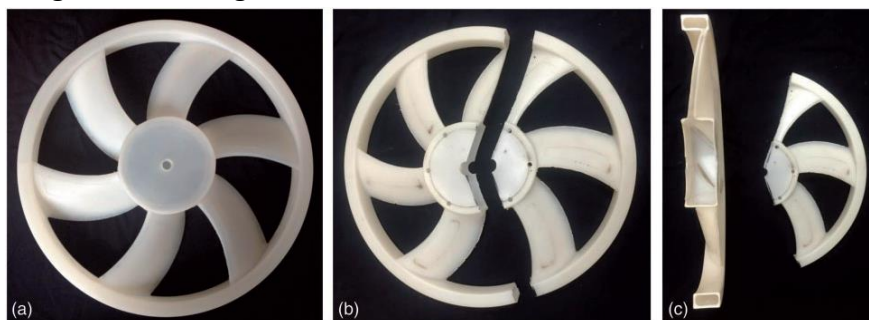
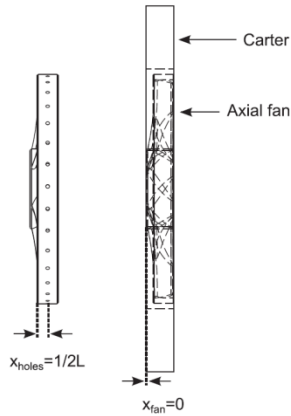


Figure 1: Hollow fan obtained with rotational molding process,

(a) the whole fan and (b), (c) the fan cut in two parts [22].



**Figure 2: on the left, position of the injection holes on the shroud ring, on the right, Position of the fan in the carter**

**Test bench and drive system**

The drive system and the test bench was reported in [22, 23]. In brief, figure 3 present the test bench used to determine the global performance which is built at the

LIFSE laboratory of Arts et Metiers Institute of Technology and developed according to the ISO-5801 standard. The airflow rate is set and measured according to ISO-5167 norm. The elevation pressures are measured with an absolute precision of 0.1 Pa. For the torque, the uncertainty of the measurements is 0.1% of the full scale equal to 5 N.m.

Initially, in order to investigate the behavior of the fan over a wide range of operating flow conditions, ten diaphragm diameters are tested (Table 1). The measurements taken show that for a diameter  $\Phi \geq 238 \text{ mm}$  the aeraulic power exhibits notable improvements in proportion to the diameters of the diaphragm.

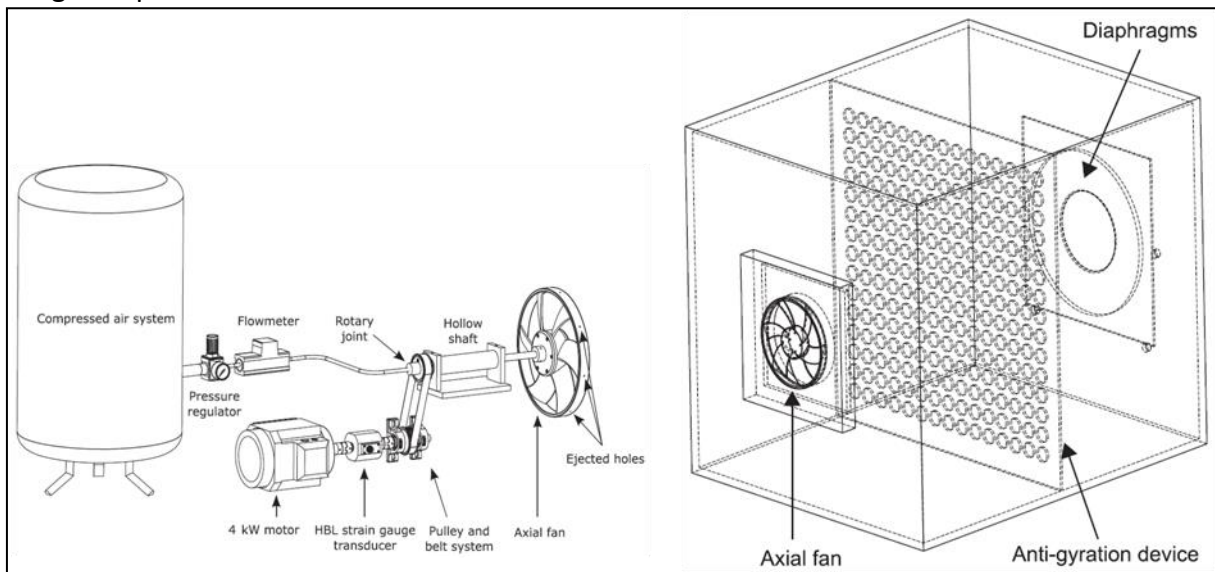


**Figure 3: Experimental setup : (a) the fan drive system, (b) ISO-5801 test bench (dimensions 1.3mx1.3mx1.8 m).**

**Table 1: Diaphragm’s diameters tested.**

$\Phi$ (mm)	77	151	169	190	220	238	267	300	336	375
-------------	----	-----	-----	-----	-----	-----	-----	-----	-----	-----

**Torque measurement:**

The experimental set-up carried out herein, the different components used for the mechanical transmission such as the motor shaft, coupling, torque meter, belt,

pulley, bearing, rotary joint generate an elementary resistive torque, hence it is difficult to estimate them separately. Our goal is to characterize the operation of the fan alone for the different control

configurations to get the static efficiency. For a given speed of rotation, this amounts to estimating its resistive torque. To do this, we proceeded first to determine the two torques, at no load  $C_0$  (fan removed) and that in presence of fan denoted by  $C$ . The net torque will then be given as follow:

$$C_{net} = C - C_0$$

During the tests, we noticed that the no-load torque  $C_0$  depends on the engine speed and the injection rate. The figure 4 below shows that for 1500 and 2000 rpm, the couple  $C_0$  stabilizes from an injection rate in the order of ( $\xi = 0.4$ ). It can be said that there is a saturation of the internal friction generated in the two rotating parts of the mechanical circuit (including the rotary joint and the hollow shaft). However, this phenomenon is not yet achieved for a rotation speed of 1000 rpm.

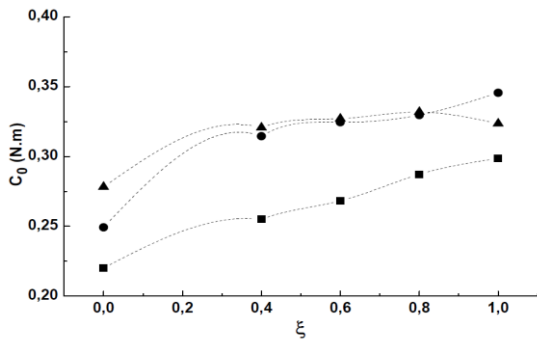


**Figure 4: No-load torque variation  $C_0$  : (■) 1000 rpm, (●) 1500 rpm, (▲) 2000 rpm.**

### CFD modeling and grid generation

The research carried out in numerical modeling has shown that it is difficult to determine all the structures generated in the flow, because it requires time and heavy computational resources. In the field of rotary flows, to simplify the problem, the periodicity condition is often used in order to carry out a detailed study on the area of interest.

On the other hand, with reference to our experimental study, the periodicity

studying a single blade is not applicable due to the number of holes used (16).

However, in order to compare the experimental results obtained with those of the CFD, it was judged that it is preferable to study the complete geometry of the test bench. In order to estimate the size of the grid of the complete domain, the geometric parameters will be deduced from the study of the sensitivity of the mesh carried out for the 1/6 of the complete domain considered as cylindrical shape. The study of the mesh is not presented in this work.

The generation of structured mesh presents a particular difficulty in the areas close to the settling chamber, the hollow area of the fan and especially at the level of the injection holes. For this, we opted for a polyhedral mesh recognized by these advantages. The refinement criteria were carried out with appropriate control volumes size (boundary layer, wake, pressure gradients...). Figure 6 presents the complete numerical domain generated in polyhedral mesh.

In our work, we use ANSYS-Fluent code with the finite volume discretization. Our approach is based on the study of the steady viscous incompressible flow with  $k - \omega$  SST turbulent model. The Moving Reference Frame (MRF) or Frame motion method is used to model the fan motion. For velocity-pressure coupling, SIMPLE algorithm is used with MUSCL Third order for the momentum equation and the second order for the rest of equations. For boundary conditions, both of inlet and outlet are maintained at atmospheric pressure. For the controlled flow configuration, the air injection is defined by mass flow inlet condition inside the hub as shown in figure 7.



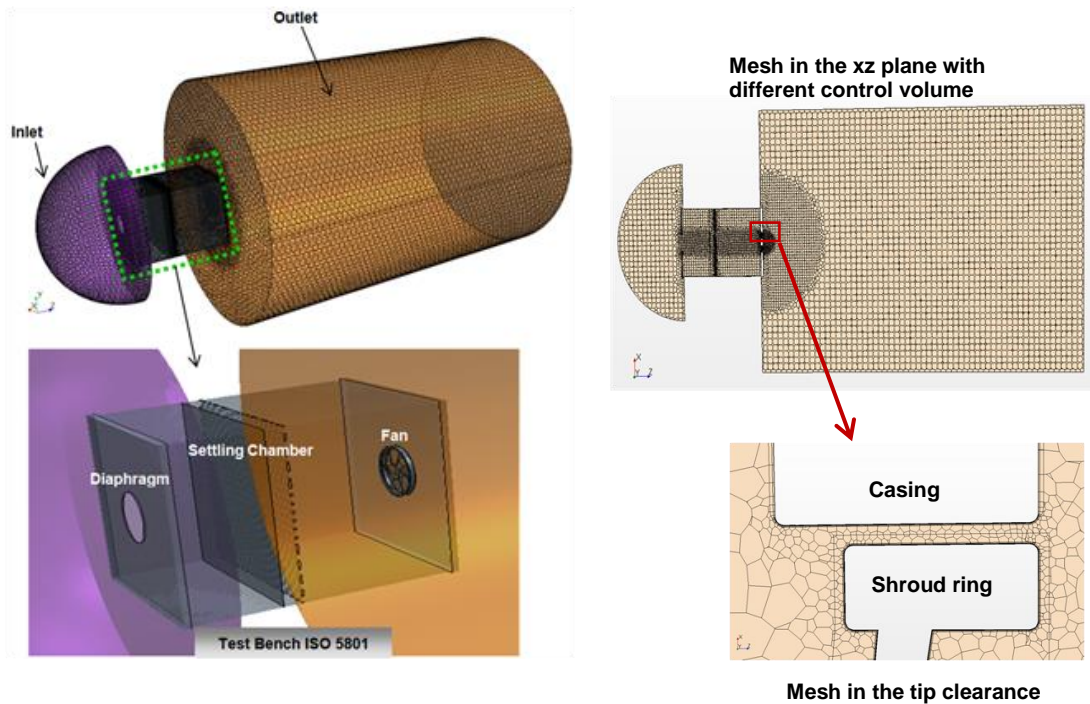


**Figure 6: Grid generation for the test bench ISO 5801**

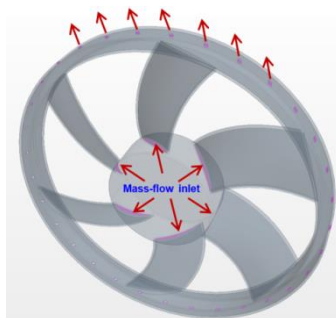


**Figure 7: Mass flow rate Boundary condition for air injection in the inside hub**

## **RESULTS**

The main findings are presented in term of gain in fan power, torque and leakage flow for the following operation conditions: 16 injection holes, two rotation speeds rpm=1000 rpm and 2000 rpm and two injections rate  $\xi = 0.4$  and 0.8.

### **Aeraulic power:**

We define the power gain as follow:  $Gain = (P - P_0)/P_0$ , where  $P = q_v \Delta P$  is the delivered power for the controle configuration and  $P_0$  is the power delivered for  $q_{inj} = 0$ .

We discussed the influence of the diaphragm diameter, rotationnal speed

and the number of the injection holes (16 and 32) where the active control improves the delivered power nearly up to 40% [22,23]. Other measurements carried out for a series of fans have shown that the optimum gain in fan power varies between 30% and 53%. This wide range of variation results mainly from the operating conditions of the rotational molding and from the manufacturing defects of the fan. The figure 5 shows the maximum gain (53%) obtained for diameter diaphragm of  $\Phi = 375 \text{ mm}$ , rotation speed of 1000 rpm and 16 injection holes.

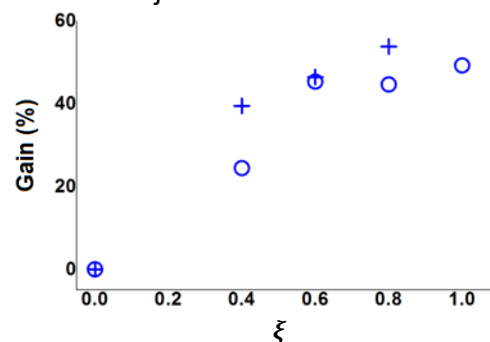


**Figure 5: Experimental results The power gain added by the control for : diaphragm diameter  $\Phi = 375 \text{ mm}$ , rotation speed 1000 rpm, +: results for 16 injection holes. o: results for 32 injection holes.**



**Resistant torque:**

Figure 8 shows the evolution of the torque developed by the fan for numerical and experimental cases. The values obtained are practically low for the two rotational speeds and seem independent of the diaphragm diameter  $\Phi$ . However, with a high speed of rotation, these low values have a significant influence on the motive power and therefore the static efficiency.

From the obtained results for the experimental study it is possible to conclude that for a control by 16 holes a maximum reduction of the torque of about 19% is reached for the speed conditions of 1000 rpm, of the diameter  $\Phi = 300$  mm and of the injection rate  $\xi = 0.8$ . The explanation is that the fan is in a rotating sprinkler configuration. The torque becomes important for a high speed of rotation (2000 rpm). In the operating tip clearance, friction remains predominant because the contribution of the blowing in terms of reducing the resistive torque remains minimal.

In the numerical simulation, the maximum torque reductions are estimated at :

- ✓ 80% for (1000 rpm,  $\xi = 0.8$  and independently of the diaphragm diameter).
- ✓ 8% for (2000 rpm,  $\Phi = 300$  mm and  $\xi = 0.8$ ).

It is noted that the gain in torque obtained experimentally (19%) is relatively low compared to the value of the gain resulting from the simulation (80%). This could be due to several experimental factors including:

- Sensitivity of the torque meter used (HBM 5 N.m). The measurement range seems important relative to the values that have been measured which are quite small. It is desirable to equip the experimental setup with a more suitable torque meter. In addition, the measurements are not direct due to the size constraint of the assembly. The

possibility of positioning the torque meter upstream of the fan (inside the box) has been abandoned due to disturbances induced in the upstream suction flow. In the event that the assembly is carried out downstream of the fan, the torque meter must be equipped with a hollow shaft (to ensure the control of the main flow) with sealed couplings to remedy leaks in the injection flow.

- Difficulty in determining the elementary torques of assembly components (belt transmission, coupling, rotating joint, etc.). We considered the net torque approach (without and with fan) with the hypothesis that with or without control, the elementary torques remains invariable.

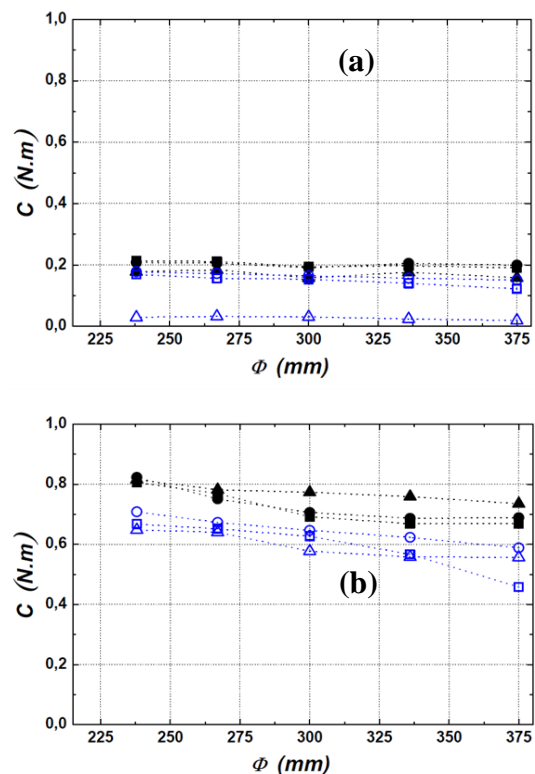


**Figure 8: Evolution of the fan torque:**  
**(a) 1000 rpm et (b) 2000 rpm.**  
**Experimental results (■) baseline, (●)  $\xi = 0.4$ , (▲)  $\xi = 0.8$ ,**  
**CFD results (□) with control, (○)  $\xi = 0.4$ ,**  
**(△)  $\xi = 0.8$ ,**

## Leakage flow :

The reduction of the leakage flow with evaluation of its influence on the different fan powers constitutes one of the primary objectives of this study [23]. From this perspective, numerical simulation provides access to the evolution of the flow in areas with experimental measurement difficulties. The leakage rate generated in a limited space of 4 mm is a typical illustrative example, where it takes sources from air deviation at the exit blade or the aspiration from the stagnation ambient air. In our work, this flow is calculated at 25% at the exit surface of the leakage flow as shown in figure 9.

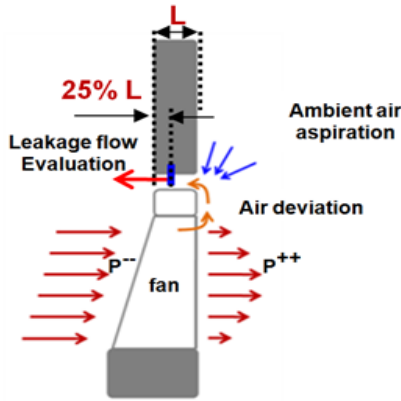


**Figure 9: leakage flow, evaluation and these sources**

In order to estimate the inherent variation of this flow relative to the nominal case, we define the gain in leakage flow as follows:

$$E_{\tau}(\%) = 100 \cdot \frac{(\dot{m}_{gap_0} - \dot{m}_{gap})}{\dot{m}_{gap_0}}$$

Where  $\dot{m}_{gap_0}$ , is the leakage flow rate calculated for the nominal case and  $\dot{m}_{gap}$  for the controlled case.

From the two figure 10, the results are presented as follows:

- For the speed of 2000 rpm and an injection rate of  $\xi = 0.4$ , a specific reduction of about 20% of the leakage flow.
- For the rest of the curves relating to the cases checked, a reduction between 50% and 80% of the leakage rate is achieved. The maximum reduction is obtained for low rotation speed (1000 rpm) and high injection rate  $\xi = 0.8$

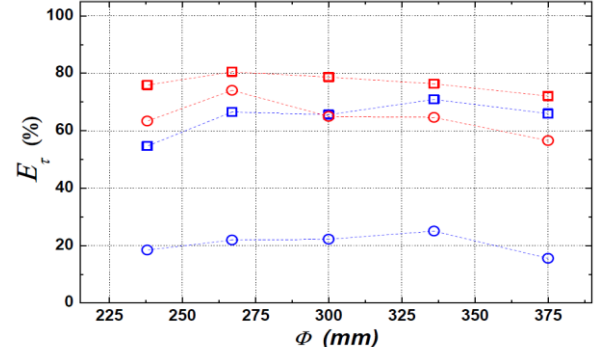


**Figure 10: Evolution of the gain in leakage flow by simulation (16 injection holes):**

**1000 rpm :** (□)  $\xi = 0.4$ , (◻)  $\xi = 0.8$ ,

**2000 rpm :** (○)  $\xi = 0.4$ , (◉)  $\xi = 0.8$ ,

It can be seen from figure 11 characterizing the nominal case, that the leakage flow behavior at tip clearance as well as both of upstream and downstream of the fan, is with high complexity including intense zones of swirling motion.

Whereas, when the flow control is imparted to the fan (figure 12) at the flow conditions  $\xi = 0.8$ , rotation speed 2000 rpm and diaphragm diameter  $\Phi = 375$  mm, important phenomenon is observed at the tip clearance between the casing and the shroud ring at the injection zone. It consists of two dead counter-rotating air regions leading to formation of two eddies besides the injection stream. Resulting in a blockage of the ambient air aspiration toward the fan portside induced by the pressure drop (figure 9).

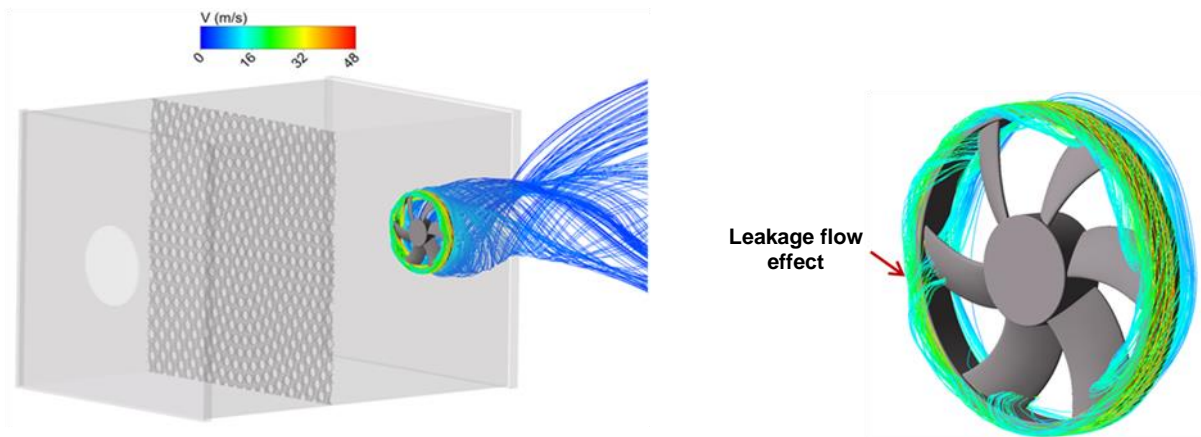


**Figure 11: Flow structure near the leakage gap, rotation speed 2000 rpm, diaphragm diameter  $\Phi = 375$  mm,**

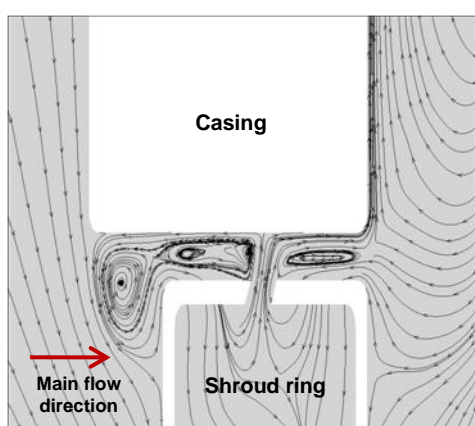


**Figure 12: Flow structure for control case near the jet at the meridian plan, rotation speed 2000 rpm, diaphragm diameter  $\Phi = 375$  mm and  $\xi = 0.8$ .**

## Conclusion

An automotive cooling fan was built with rotational molding process which induces a hollow shape for the whole fan. This latter is used to drive air injection from hub to the tip clearance through a shroud ring to control the leakage flow, which is considered a source of energy dissipation. The internal flow generated by a specific drive system exits at the fan periphery by 16 holes. Numerical and experimental studies were carried out, especially in this study, for the two rotational speeds 1000 rpm and 2000 rpm, and two injections rate  $\xi = 0.4$  and  $0.8$ .

In experiment, after a series of tests on rotomolded fans, the obtained results

show that the maximum gain in fan power is about 53%. The variation of this maximum is related to the operating conditions of the rotational molding process and its manufacturing defects.

For both studies, CFD and experiment, the control by air injection leads to an improvement in terms of reducing of leakage flow rate and fan torque.

With CFD, we reach reduction about 80% for leakage flow rate and torque at low rotation speed 1000 rpm and high injection rate  $\xi = 0.8$ . However, for the experimental, the gain in torque reduction is about 19% which is relatively low compared to the numerical result.

As perspectives, the authors plan to consider the effect of the rotational molding process parameters to further improve the gain in fan power. Also, try to estimate the gain in torque especially in the presence of the internal flow with the remaining parts of the drive system.

## References

1. Boudet J, Cahuzac A, Kausche P, et al. Zonal large eddy simulation of a fan tip-clearance flow, with evidence of vortex wandering. *J Turbomach* 2015; 137(6): 061001.
2. Fischer A, König J, Czarske J, et al. Investigation of the tip leakage flow at turbine rotor blades with squealer cavity. *Exp Fluid* 2013; 54(2): 1–15.
3. Pogorelov A, Meinke M and Schröder W. Effects of tip gap width on the flow field in an axial fan. *Int J Heat*

Fluid Fl 2016; 61: 466–481.

4. You D, Wang M, Moin P, et al. Effects of tip-gap size on the tip-leakage flow in a turbomachinery cascade. *Phys Fluid* 2006; 18(10): 105102.

5. Lee S, Kim S and Kim K. Aerodynamic performance of winglets covering the tip gap inlet in a turbine cascade. *Int J Heat Fluid Fl* 2012; 34: 36–46.

6. Wallis A, Denton J and Demargne A. The control of shroud leakage flows to reduce aerodynamic losses in a low aspect ratio, shrouded axial flow turbine. *J Turbomach* 2001; 123(2): 334–341.

7. Corsini A, Rispoli F and Sheard A. Development of improved blade tip endplate concepts for low-noise operation in industrial fans. *Proc IMechE Part A J Pow* 2007; 221(5): 669–681.

8. Akturk A and Camci C. Axial flow fan tip leakage flow control using tip platform extensions. *J Fluid Eng* 2010; 132(5): 051109.

9. Pardowitz B, Moreau A, Tapken U, et al. Experimental identification of rotating instability of an axial fan with shrouded rotor. *Proc IMechE Part A J Pow* 2015; 229(5): 520–528.

10. Longhouse R. Control of tip-vortex noise of axial flow fans by rotating shrouds. *J Sound Vib* 1978; 58(2): 201–214.

11. Vad J, Horva' th C and Kova' cs J. Aerodynamic and aero-acoustic improvement of electric motor cooling equipment. *Proc IMechE Part A J Pow* 2014; 228(3): 300–316.

12. Weigl H, Paduano J, Frechette L, et al. Active stabilization of rotating stall and surge in a transonic single stage axial compressor. In: ASME 1997 international gas turbine and aeroengine congress and exhibition.

13. Rhee S, Kim S, Ahn H, et al. Analysis of a jet controlled high-lift hydrofoil with a flap. *Ocean Eng* 2003; 30(16): 2117–2136.

14. Eberlinc M, S' irok B and Hoc'var M. Experimental investigation of the interaction of two flows on the axial fan hollow blades by flow visualization and hot-wire anemometry. *Exp Therm Fluid Sci* 2009; 33(5): 929–937.

15. Eberlinc M, S' irok B, Dular M, et al. Modification of axial fan flow by trailing edge self-induced blowing. *J Fluid Eng* 2009; 131(11): 111104.

16. Eberlinc M, S' irok B, Hoc'var M, et al. Numerical and experimental investigation of axial fan with trailing edge self-induced blowing. *Forsch Ingenieurwes* 2009; 73(3): 129–138.

17. Neuhaus L and Neise W. Active control to improve the aerodynamic performance and reduce the tip clearance noise of axial turbomachines with steady air injection into the tip clearance gap. In: King R (ed.) *Active flow control (Notes on Numerical*

*Fluid Mechanics and Multidisciplinary Design*. vol. 95, Berlin/Heidelberg: Springer, 2007, pp.293–306.

18. Morris S.C and Foss J.F. An aerodynamic shroud for automotive cooling fans. *Journal of fluids engineering*, 123(2) :287-292, 2001.

19. Niu M and Zang S. Experimental and numerical investigations of tip injection on tip clearance flow in an axial turbine cascade. *Exp Therm Fluid Sci* 2011; 35(6): 1214–1222.

20. Wadia A and Szucs P. Inner workings of shrouded and unshrouded transonic fan blades. *J Turbomach* 2008; 130(3): 031010.

21. Sarraf C, Nouri H, Ravelet F, et al. Experimental study of blade thickness effects on the overall and local performances of a controlled vortex designed axial flow fan. *Exp Therm Fluid Sci* 2011; 35(4): 684–693..

22. Azzam T, Paridaens R, Ravelet F, Khelladi S, Oualli H and Bakir F. Experimental investigation of active control by steady air injection in the tip clearance gap of an axial fan. *International Symposium on Transport Phenomena and Dynamics of Rotating Machinery (ISROMAC 2016)*. April 10-15, 2016, Hawaii, Honolulu

23. Azzam T, Paridaens R, Ravelet F, Khelladi S, Oualli Hand Bakir F. Experimental investigation of an actively controlled automotive cooling fan using steady air injection in the leakage gap. *Proc IMechE Part A: J Power and Energy* 2017, Vol. 231(1) 59–67.

24. C. Sarraf, H. Nouri, F. Raveleta, F. Bakir. Experimental study of blade thickness effects on the overall and local performances of a Controlled Vortex Designed axial-flow fan. *Journal Experimental Thermal and Fluid Science*, 2011.